Case Report

Enhanced magnetic resonance imaging features and management principles of low-grade myofibroblastic sarcoma of the breast: a case report

Meng Zhu[1], Wei Cheng[2], Xuejuan Liu[3], Lin Ma[1], Yujuan Chen[3]

[1]Department of Ultrasound, West China Hospital of Sichuan University, Chengdu, China; [2]Department of Radiology, West China Hospital of Sichuan University, Chengdu, China; [3]Department of Breast Disease Center, West China Hospital of Sichuan University, Chengdu, China

Contributions: (I) Conception and design: M Zhu, W Cheng, Y Chen; (II) Administrative support: Y Chen, L Ma; (III) Provision of study materials or patients: M Zhu, X Liu, W Cheng; (IV) Collection and assembly of data: M Zhu, X Liu, W Cheng, L Ma; (V) Data analysis and interpretation: M Zhu, W Cheng; (VI) Manuscript writing: All authors; (VII) Final approval of manuscript: All authors.

Correspondence to: Wei Cheng, MS. Department of Radiology, West China Hospital of Sichuan University, No. 37 Guoxuexiang Road, Chengdu 610041, China. Email: chengwei5556@wchscu.cn; Yujuan Chen, MD. Department of Breast Disease Center, West China Hospital of Sichuan University, No. 37 Guoxuexiang Road, Chengdu 610041, China. Email: chenyujuan@wchscu.cn.

Background: Low-grade myofibroblastic sarcoma (LGMS) originating from breast is rare. Existing literature comprises clinical and pathological reports, with limited information on imaging characteristics. This study reports a case of LGMS of the breast and presents its imaging characteristics, with an emphasis on those observed using contrast-enhanced magnetic resonance imaging (MRI).

Case Description: A 50-year-old patient presented with a left breast mass for 1 year. One year before the presentation, the patient had palpated a mass of approximately 1.5 cm in size in the upper part of the left breast without any obvious cause. The mass was perceived to be growing slowly. There was no relevant family history of breast conditions. Physical examination revealed a hard, ill-defined, irregularly shaped, non-tender mass of approximately 3.5 cm × 3 cm in size, with poor mobility and a close connection to the deep skin. The mammography showed a high-density mass without microcalcifications and boundary wrapping. Ultrasonography showed an oval, ill-defined hypoechoic mass. The combination of mammography and ultrasound examination results ruled out the possibility of ductal carcinoma and benign fibroepithelial tumor. On contrast-enhanced MRI, the mass exhibited heterogeneous enhancement, high signal intensity on T2-weighted imaging (T2WI), high signal intensity on diffusion-weighted imaging (DWI), and a type I time-intensity curve (TIC). A core needle biopsy (CNB) suggested a spindle cell tumor. To confirm the diagnosis, the patient underwent surgical excision, and postoperative pathology confirmed LGMS of the breast. The patient subsequently received adjuvant radiotherapy. Seven months postoperatively, bone scintigraphy suggested possible metastases.

Conclusions: LGMS of the breast exhibited a degree of malignancy on ultrasonography, mammography, and MRI, with the contrast-enhanced MRI showing a persistent enhancement pattern (type I TIC). A preoperative biopsy indicated a spindle cell tumor. Surgical excision remains the best diagnostic method. A thorough understanding of the imaging characteristics and biopsy results of this tumor type provides comprehensive information for formulating corresponding treatment plans.

Keywords: Breast; myofibroblastic sarcoma; contrast-enhanced magnetic resonance imaging (contrast-enhanced MRI); case report

Submitted Aug 13, 2024. Accepted for publication Jan 02, 2025. Published online Jan 20, 2025.
doi: 10.21037/gs-24-347
View this article at: https://dx.doi.org/10.21037/gs-24-347

Introduction

Low-grade myofibroblastic sarcoma (LGMS) is a spindle cell tumor originating from myofibroblasts (1-3). These tumors are more commonly found in the head and neck region, particularly in the oral cavity (2,4). Clinically, they present as painless enlarging masses with an infiltrative growth pattern (2). The 2020 updated World Health Organization classification system for fibroblastic and myofibroblastic tumors lists LGMS as a separate entity (intermediate, rarely metastasizing), distinguishing it from other benign and malignant entities (5,6).

LGMS originating from the breast is rare, and preoperative imaging diagnosis of LGMS is relatively difficult (7-11). Puncture biopsy has a positive diagnostic effect, but it has limitations, and the final diagnosis relies on pathology (7-9,11). Surgical resection is usually the main treatment method for LGMS, and the prognosis of most patients is favorable (2). A few case reports in the English literature have described the imaging (mammography and ultrasound) characteristics of LGMS of the breast. However, to our knowledge, the perfusion curve type of LGMS of the breast on contrast-enhanced magnetic resonance imaging (MRI) has not been reported. Therefore, this study presents the imaging characteristics of a case of LGMS of the breast, with a focus on the characteristics of contrast-enhanced MRI and the dynamic perfusion curve type. The study aimed to provide a comprehensive understanding of this tumor type, facilitating clinical decision-making. We present this case in accordance with the CARE reporting checklist (available at https://gs.amegroups.com/article/view/10.21037/gs-24-347/rc).

Highlight box

Key findings

- Low-grade myofibroblastic sarcoma (LGMS) appeared as an oval-shaped, ill-defined hypoechoic mass on ultrasonography. Mammography revealed an irregular, high-density mass. Contrast-enhanced magnetic resonance imaging (MRI) showed heterogeneous enhancement, high signal on T2-weighted imaging, high signal on diffusion-weighted imaging, and a dynamic enhancement curve indicating a persistent phase with a type I time-intensity curve.

What is known and what is new?

- LGMS is a distinct entity clinically characterized by painless palpable masses. The imaging features of LGMS lack specificity and overlap with other types of benign and malignant breast tumors, making differential diagnosis difficult.
- In this case, we described in detail, the multimodal imaging features of LGMS, particularly the MRI findings, providing imaging evidence.

What is the implication, and what should change now?

- LGMS presents with atypical clinical manifestations and imaging features that require careful consideration. When differentiation proves challenging, core needle biopsy can facilitate diagnosis.

Case presentation

A 50-year-old patient presented to the authors' hospital with a left breast mass for 1 year. One year before the presentation, the patient had palpated a mass of approximately 1.5 cm in size in the upper part of the left breast without any obvious cause. The patient reported no redness, pain, nipple discharge, weight loss, night sweats, or other discomfort and had not sought treatment. The mass was perceived to be growing slowly. There was no relevant family history of breast cancer or history of surgery.

Physical examination revealed asymmetry between the breasts, with a slight elevation at the 12 o'clock position, approximately 4 cm from the left nipple. A hard, ill-defined, irregularly shaped, non-tender mass of approximately 3.5 cm × 3 cm in size was palpable beneath the elevated area, with poor mobility and a close connection to the deep skin. No mass was palpable in the right breast. Compression of the left nipple revealed a small amount of cloudy, light-yellow discharge from a single duct on the lateral side of the nipple, whereas no discharge was observed from the right nipple. No significant lymph node enlargement was palpable in the bilateral axillae and the supraclavicular and infraclavicular areas.

Mammography of the breast showed a partially obscured mass with some margins visible (approximately 2.0 cm × 1.7 cm) (*Figure 1*). The patient also underwent an ultrasound examination, which revealed a hypoechoic, heterogeneous solid mass with indistinct borders measuring approximately 30 mm × 13 mm × 20 mm. The mass was located at the 12 o'clock position, approximately 4 cm from the left nipple, and involved the subcutaneous layer (*Figure 2A*). According to the Breast Imaging Reporting and Data System (BI-RADS) classification, this lesion is considered to be in the 4C category (12). Color Doppler ultrasound showed blood supply within the mass (*Figure 2B*). Multiple solid nodules were observed in the remaining areas of both breasts (BI-RADS category 3).

For more information about the mass, the patient underwent a contrast-enhanced breast MRI. Images

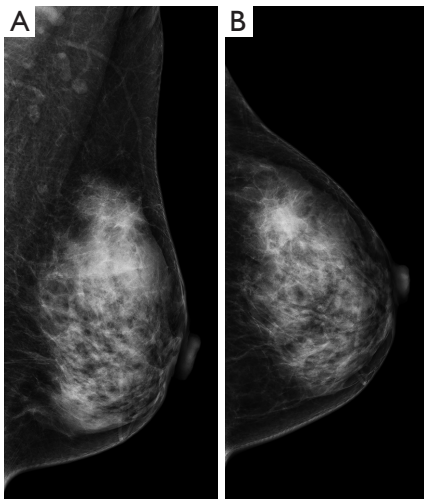

Figure 1 Radiographic examination results. (A,B) The mammography showed a high-density mass with obscured boundaries: (A) mediolateral oblique view; (B) craniocaudal view.

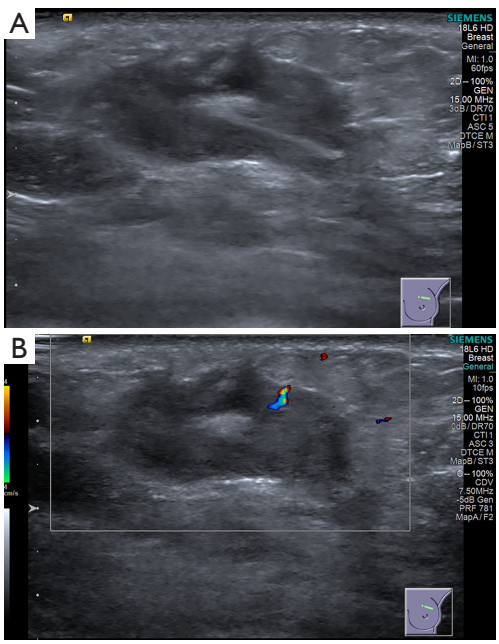

Figure 2 Two-dimensional and color Doppler ultrasound images of mass. (A) Left breast features a hypoechoic mass approximately 30 mm × 13 mm × 20 mm in size at the 12 o'clock position, with unclear borders and irregular shape. The internal echogenicity of the mass is heterogeneous, with only slight hypoechogenicity visible. (B) Color Doppler ultrasound displays a prominent thick vessel within the tumor.

were acquired using a GE Healthcare (Architect) 3.0-T MRI system (GE Healthcare, Chicago, IL, USA) with a dedicated 16-channel breast coil. The dynamic contrast-enhanced MRI protocol involved six continuous scans, each lasting 1 minute and 23 seconds, for a total scan time of approximately 9 minutes. A Bayer high-pressure injector was employed to administer the contrast agent (gadopentetate dimeglumine) at a rate of 3 mL/s, with a total volume of 0.2 mL/kg. Time-signal curve analysis was performed using GE Gen IQ software. The contrast-enhanced MRI revealed an oval-shaped, spiculated, heterogeneously enhancing mass in the upper quadrant of the left breast (*Figure 3A*). The lesion measured approximately 2.3 cm (anteroposterior) × 2.2 cm (mediolateral) × 2.8 cm (superoinferior). It displayed isointensity on T1-weighted imaging (T1WI), hyperintensity on T2-weighted imaging (T2WI) (*Figure 3B*), and hyperintensity on diffusion-weighted imaging (DWI) (*Figure 3C*), apparent diffusion coefficient map showed restricted diffusion (*Figure 3D*). Subsequently, the most suspicious areas were manually contoured as the region of interest to generate dynamic enhancement curves. The initial phase of enhancement was rapid, whereas the delayed phase showed persistent enhancement, with the overall dynamic enhancement curve exhibiting a persistent phase (*Figure 3E*). Preoperative ultrasound-guided biopsy indicated a spindle cell tumor, suggesting the necessity of complete surgical excision for a definitive diagnosis.

To confirm the diagnosis, the surgeon and patient had a detailed discussion and designed a personalized treatment plan. Owing to the high malignancy risk, surgery was the preferred treatment. The patient underwent a left breast tumor resection, including the relevant lymph node dissection. Intraoperatively, a 3.5 cm × 3 cm hard, ill-defined, infiltrative mass without a capsule was found at the 12 o'clock position of the left breast. Frozen section analysis indicated a spindle cell tumor, with no tumor involvement at the "upper, lower, inner, outer, and basal margins" of the specimen. Additionally, the same sections revealed no tumor involvement of sentinel lymph nodes 1–5 in the left breast.

After resection, the tumor underwent postoperative pathological examination (*Figure 4*). The results confirmed invasive tumor growth infiltrating the adipose tissue (*Figure 4A*). The tumor cells were spindle-shaped with moderate atypia (*Figure 4B*,*4C*) and a low mitotic rate (fewer than 5 per 10 high-power fields) (*Figure 4D*). Focal

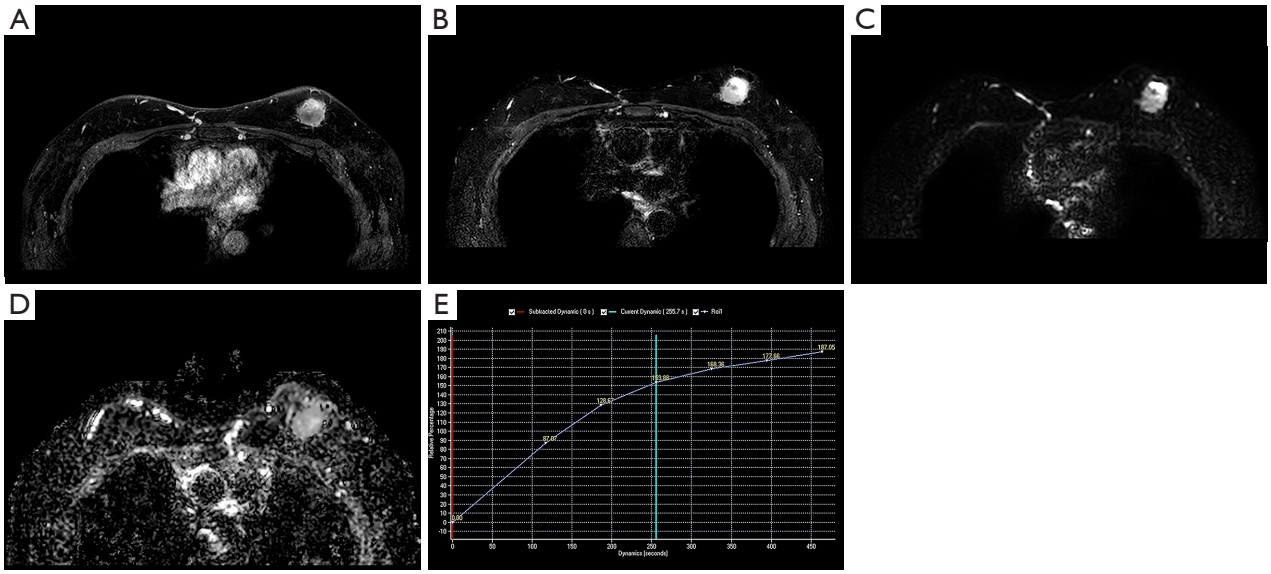

Figure 3 MRI images and dynamic perfusion curve. (A) Transverse T1 fat-suppressed contrast-enhanced scan shows heterogeneous enhancement of the lesion. (B) A T2-weighted fat-suppressed image shows a high signal in the lesion. (C) DWI. (D) Apparent diffusion coefficient map. (E) Dynamic contrast-enhanced perfusion curve. MRI, magnetic resonance imaging; DWI, diffusion-weighted imaging.

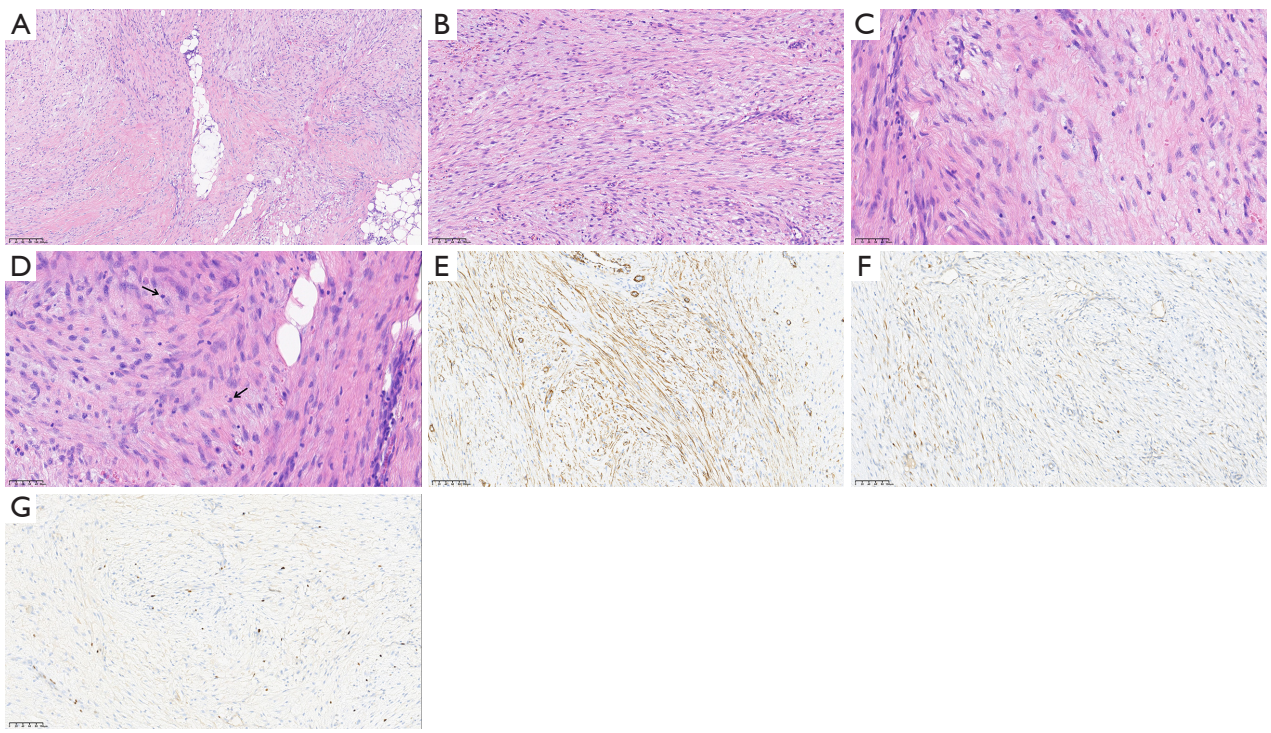

Figure 4 Pathological examination results of the lump. (A-D) Hematoxylin-eosin staining. (A) The tumor exhibits invasive growth and infiltrates surrounding adipose tissue (×100). (B) Spindle-shaped tumor cells are arranged in interwoven bundles (×200). (C) Tumor cells with moderate atypia (×400). (D) A few mitotic figures are indicated by black arrows (×400). (E-G) Immunohistochemical staining. (E) Smooth muscle actin shows positive results (partially+) (×200). (F) Desmin shows positive results (focally+) (×200). (G) The Ki-67 positive index is 5% (×200).

areas showed myxoid changes. Immunohistochemistry results indicated SMA (partial+) (*Figure 4E*), desmin (focal+) (*Figure 4F*), beta-catenin (nuclear–), MyoD1 (–), Myogenin (–), S100 (–), MUC4 (–), H3 K27Me3 (no loss), CD34 (–), EMA (–), TLE1 (–), and Ki-67 (MIB-1) (5% positivity) (*Figure 4G*).

Molecular pathology tests included polymerase chain reaction (PCR)-*CTNNB1/APC* mutation analysis (no hotspot mutations detected). Fluorescence in situ hybridization (FISH) analysis detected no *FUS* gene rearrangement nor *MDM2* gene amplification. The patient was diagnosed with fibroblastic/myofibroblastic tumor, specifically LGMS [French Federation of Cancer Centers Sarcoma Group (FNCLCC) grade 1 (G1)] (13), with no tumor involvement at the resection margins using histology, immunohistochemistry, and genetic testing.

Considering that the patient underwent breast-conserving surgery and the tumor had low malignancy (FNCLCC: G1), the patient had detailed communication with the oncologist and received local radiation therapy. The treatment was divided into two stages: phase 1, 25 radiotherapy sessions, total dose: 5,000 Cgy; phase 2, 5 radiotherapy sessions, total dose: 1,000 Cgy. At 7 months post-surgery, bone scintigraphy indicated elevated metabolic activity in the left 6th rib (axillary segment) and the 9th thoracic vertebra. The patient continued with radiotherapy according to the treatment plan. During the 13-month postoperative follow-up, the patient's chest CT and whole-body nuclear medicine bone imaging did not show any further progression of the condition. All procedures performed in this study were in accordance with the ethical standards of the institutional and/or national research committee(s) and with the Helsinki Declaration (as revised in 2013). The work was approved by the Ethics Committee of West China Hospital of Sichuan University [2024 Audit (No. 1438)]. Publication of this case report and accompanying images was waived from patient consent according to the West China Hospital of Sichuan University ethics committee review board.

Discussion

This study presents a case of LGMS of the breast with multiple nodules in bilateral breasts and highlights the imaging characteristics of the lesion, particularly the dynamic contrast-enhanced MRI features and perfusion curve type. These features require differentiation from various solid breast tumors.

According to a literature review by Deng *et al.*, wherein approximately 20 cases of myofibroblastic sarcoma were included (11), some cases had spindle cells detected through preoperative biopsy. Among these, two cases showed atypical spindle cells [one had numerous mitotic figures (7), while the other suggested sarcoma (9)]. Myong *et al.* initially suspected fibroadenoma based on imaging, but biopsy revealed myofibroblastoma (8). In another case reported by Deng *et al.*, core biopsy results indicated low-grade spindle cell sarcoma with necrosis (11). In the present case as well, biopsy only revealed a small number of spindle cell tumors. This indicates that biopsy alone has limitations in determining the specific tumor pathology. Intraoperative frozen section analysis can confirm the tumor nature and surgical margin condition and can be supplemented by sentinel lymph node biopsy when necessary.

The imaging manifestations of LGMS are described as follows: Morgan *et al.* reported one case with lobulated mass with partially defined edges on mammography (7), and two cases with well-defined high-density masses (8,9). Myong *et al.* described an LGMS case arising from fibroadenoma, stating that the lesion appeared as a well-defined mass that might be masked by the imaging characteristics of fibroadenoma (8). Scardina *et al.* (9) reported it as a hypoechoic nodular mass with a capsule on ultrasonography. Wang *et al.* (10) described it as a high-density, well-defined lobulated mass. Deng *et al.* (11) reported it as a hypoechoic irregular mass on ultrasonography.

In the present case, multiple breast nodules resulted in potentially overlapping masses on mammography, which, together with dense glandular tissue, made the edges difficult to identify, thereby necessitating further evaluation with ultrasound or MRI.

In the case presented in this report, the lesion exhibited heterogeneous high signal intensity on T2WI and low-to-intermediate signal intensity on T1WI, demonstrating uneven enhancement. This can be attributed to the presence of a mucinous matrix or necrotic components, which display high signal intensity on T2-weighted MRIs. Lesions with dense cellularity and collagen content exhibit lower signal intensity on MRIs but may appear hyperechoic on ultrasonography (14). A case of radiation-induced LGMS reported in the literature also showed heterogeneous enhancement on MRI (15). Notably, the dynamic enhancement curve of this patient's LGMS was consistent with the curves of other nodules in the same breast, presenting a persistent phase, which can be misleading and warrants caution. This dynamic enhancement pattern of LGMS in the

breast has not been previously described. In contrast, the dynamic enhancement curves of typical breast cancers are dominated by plateau or washout phases (type II or III) (16). Benign-enhancing lesions, however, display a steadily progressive signal intensity over time (type I). An apparent diffusion coefficient value of less than 1.1×10^{-3} mm^2/s also serves as a strong indicator of malignancy (17,18).

In the present case, the LGMS was complicated by multiple breast nodules, necessitating differentiation among various lesion types to identify higher-risk nodules for subsequent biopsy. The primary benign tumor that needs differentiation is fibroadenoma, which commonly occurs in young women and appears with clear boundaries and good mobility on imaging. Another essential differentiation is phyllodes tumor, which presents as a lobulated mass on imaging and has a peripheral blood supply. Other benign tumors that require differentiation include nodular fasciitis and fibromatosis. Nodular fasciitis usually occurs in the subcutaneous fat layer near the superficial fascia, and its MRI dynamic curve shows early rapid enhancement and a washout pattern (19). Alternatively, fibromatosis typically appears irregular and lobulated with heterogeneous enhancement on MRI (20). Among six patients with fibromatosis, four had type I time-intensity curve (TIC), and the others had type II or III TIC (20). The tumor may also be associated with posterior acoustic shadowing on ultrasonography.

Differentiating malignant tumors from other non-calcified breast sarcomas is crucial. Typically, these malignant tumors appear as large, oval, lobulated infiltrative masses on imaging (21), which overlap with the imaging characteristics of this case. There is a correlation between lobular structure and high expression of HIF-1α in imaging (22). Additionally, the TIC requires large sample studies for effective differentiation among various sarcoma types. When differentiation becomes challenging, biopsy results should be incorporated. For suspicious malignant lesions, a core needle biopsy (CNB) is recommended. Upon the detection of spindle cells, necrosis, or nuclear atypia in the CNB, extensive surgical excision should be considered to clarify the nature of the mass.

LGMS exhibits invasive biological behavior. Histologically, it originates from mesenchymal spindle cell differentiation. LGMS features relatively circumscribed boundaries, uniformly arranged fascicles, possible local infiltration, and nuclei with mild-to-moderate atypia, often with localized mitotic figures (23-25). Ultrastructurally, myofilaments and rough endoplasmic reticulum can be observed under electron microscopy (1,23). Myoid cell markers, including α-smooth muscle actin, muscle-specific actin, desmin, and fibronectin, aid in LGMS diagnosis (25,26). In the present case, a comprehensive diagnosis was made through careful light microscopy observation, molecular immunomarkers, and molecular biology, although electron microscopy is the ideal approach for diagnosis. There are four possible types of fibroblastic/myofibroblastic lesions: reactive (reparative lesions), benign, intermediate, and malignant tumors. Some immunohistochemical markers and molecular tests assist in determining the type and nature of fibroblast/myofibroblast tumors. The analysis of beta-catenin (nuclear–) and PCR *CTNNB1/APC* mutations, in this case, did not detect any hotspot mutations, ruling out the possibility of ligament-like fibromatosis; CD34 (–) excluded dermatofibrosarcoma protuberans and solitary fibrotic tumors; EMA (–), MUC4 (–), and FISH did not detect *FUS* gene translocation, ruling out low-grade fibromyxoid sarcoma (24,27-30).

The biological behavior assessment of tumors depends on the type of tumor itself. FNCLCC grading is an important pathological grading system used to evaluate the malignancy and prognosis of soft tissue sarcoma, with key elements including tumor differentiation, mitosis, and tumor necrosis (13). The Ki-67 index reflects the proliferative activity of tumors, and in this case, Ki-67 (MIB-1) (positive rate 5%) is consistent with FNCLCC G1. A study suggested that high-grade myofibroblastic sarcoma with necrosis or more than six mitoses per 10 high-power fields was statistically associated with a significantly elevated risk of disease-related mortality (31).

Although LGMS rarely recurs or metastasizes, long-term monitoring is essential, as the lungs and bones are the most common metastatic sites (10). The standard and efficacy of radiotherapy and chemotherapy remain unclear. Extensive local excision with adequate margins is crucial for treating LGMS, as research has indicated that cases with all margins ≥2 cm showed no recurrence during follow-up (32). Besides, as a member of the sarcoma family, personalized management may be carried out for each patient based on molecular genetic testing results and clinical conditions (33).

Conclusions

This article presents a rare case of a 50-year-old woman with breast LGMS. Calcification was absent on imaging, and MRI displayed heterogeneous enhancement with a type I curve. Puncture biopsy can facilitate diagnosis, and

the final diagnosis should rely on clinical pathology and molecular testing. Adequate excision margins are necessary for treatment in such cases.

Acknowledgments

We would like to thank Editage (https://www.editage.cn/) for English language editing.

Footnote

Reporting Checklist: The authors have completed the CARE reporting checklist. Available at https://gs.amegroups.com/article/view/10.21037/gs-24-347/rc

Peer Review File: Available at https://gs.amegroups.com/article/view/10.21037/gs-24-347/prf

Funding: This work was sponsored by the National Key Research and Development Program of China (No. 2020YFA0714002).

Conflicts of Interest: All authors have completed the ICMJE uniform disclosure form (available at https://gs.amegroups.com/article/view/10.21037/gs-24-347/coif). The authors have no conflicts of interest to declare.

Ethical Statement: The authors are accountable for all aspects of the work in ensuring that questions related to the accuracy or integrity of any part of the work are appropriately investigated and resolved. All procedures performed in this study were in accordance with the ethical standards of the institutional and/or national research committee(s) and with the Helsinki Declaration (as revised in 2013). The work was approved by the Ethics Committee of West China Hospital of Sichuan University [2024 Audit (No. 1438)]. Publication of this case report and accompanying images was waived from patient consent according to the West China Hospital of Sichuan University ethics committee review board.

References

1. Fisher C. Myofibroblastic malignancies. Adv Anat Pathol 2004;11:190-201.
2. Mentzel T, Dry S, Katenkamp D, et al. Low-grade myofibroblastic sarcoma: analysis of 18 cases in the spectrum of myofibroblastic tumors. Am J Surg Pathol 1998;22:1228-38.
3. Fisher C. Myofibrosarcoma. Virchows Arch 2004;445:215-23.
4. Giraldo-Roldan D, Louredo BVR, Penafort PVM, et al. Low-Grade Myofibroblastic Sarcoma of the Oral and Maxillofacial Region: An International Clinicopathologic Study of 13 Cases and Literature Review. Head Neck Pathol 2023;17:832-50.
5. Sbaraglia M, Bellan E, Dei Tos AP. The 2020 WHO Classification of Soft Tissue Tumours: news and perspectives. Pathologica 2021;113:70-84.
6. WHO Classification of Tumours Editorial Board. Soft Tissue and Bone Tumours. WHO Classification of Tumours, 5th Edition, Volume 3. Lyon: International Agency for Research on Cancer; 2020. Available online: https://publications.Iarc.fr/588
7. Morgan PB, Chundru S, Hatch SS, et al. Uncommon malignancies: case 1. Low-grade myofibroblastic sarcoma of the breast. J Clin Oncol 2005;23:6249-51.
8. Myong NH, Min JW. Low-grade myofibroblastic sarcoma arising in fibroadenoma of the breast-A case report. Diagn Pathol 2016;11:33.
9. Scardina L, Franceschini G, Di Leone A, et al. Low-grade myofibroblastic sarcoma of the breast. Breast J 2020;26:2077-8.
10. Wang L, Li LX, Chen DQ, et al. Low-grade Myofibroblastic sarcoma: clinical and imaging findings. BMC Med Imaging 2019;19:36.
11. Deng Z, Xia C, Li Y, et al. Myofibroblastic sarcoma in breast: a case report and literature review. Front Oncol 2024;14:1366546.
12. D'Orsi CJ, Sickles EA, Mendelson EB, et al. ACR BI-RADS® Atla. Breast Imaging Reporting and Data System. Reston: American College of Radiology; 2013. Available online: https://www.acr.org/Clinical-Resources/Reporting-and-Data-Systems/Bi-Rads
13. Coindre JM. Grading of soft tissue sarcomas: review and update. Arch Pathol Lab Med 2006;130:1448-53.

14. Haseli S, Mansoori B, Christensen D, et al. Fibroblastic and Myofibroblastic Soft-Tissue Tumors: Imaging Spectrum and Radiologic-Pathologic Correlation. Radiographics 2023;43:e230005.
15. Val-Bernal JF, Hermana S, Alonso-Bartolomé MP. Myofibroblastic sarcoma of the breast. Report of a case induced by radiotherapys. Pathol Res Pract 2019;215:152664.
16. Kuhl CK, Mielcareck P, Klaschik S, et al. Dynamic breast MR imaging: are signal intensity time course data useful for differential diagnosis of enhancing lesions? Radiology 1999;211:101-10.
17. Yabuuchi H, Matsuo Y, Okafuji T, et al. Enhanced mass on contrast-enhanced breast MR imaging: Lesion characterization using combination of dynamic contrast-enhanced and diffusion-weighted MR images. J Magn Reson Imaging 2008;28:1157-65.
18. Chen P, Zhao S, Guo W, et al. Dynamic contrast-enhanced magnetic resonance imaging features and apparent diffusion coefficient value of HER2-positive/HR-negative breast carcinoma. Quant Imaging Med Surg 2023;13:4816-25.
19. Rhee SJ, Ryu JK, Kim JH, et al. Nodular fasciitis of the breast: two cases with a review of imaging findings. Clin Imaging 2014;38:730-3.
20. Lorenzen J, Cramer M, Buck N, et al. Desmoid Type Fibromatosis of the Breast: Ten-Year Institutional Results of Imaging, Histopathology, and Surgery. Breast Care (Basel) 2021;16:77-84.
21. Smith TB, Gilcrease MZ, Santiago L, et al. Imaging features of primary breast sarcoma. AJR Am J Roentgenol 2012;198:W386-93.
22. Li X, Xie Y, Hu Y, et al. Soft tissue sarcoma: correlation of dynamic contrast-enhanced magnetic resonance imaging features with HIF-1α expression and patient outcomes. Quant Imaging Med Surg 2022;12:4823-36.
23. Krings G, McIntire P, Shin SJ. Myofibroblastic, fibroblastic and myoid lesions of the breast. Semin Diagn Pathol 2017;34:427-37.
24. Magro G, Salvatorelli L, Puzzo L, et al. Practical approach to diagnosis of bland-looking spindle cell lesions of the breast. Pathologica 2019;111:344-60.
25. Meng GZ, Zhang HY, Bu H, et al. Myofibroblastic sarcomas: a clinicopathological study of 20 cases. Chin Med J (Engl) 2007;120:363-9.
26. Qiu X, Montgomery E, Sun B. Inflammatory myofibroblastic tumor and low-grade myofibroblastic sarcoma: a comparative study of clinicopathologic features and further observations on the immunohistochemical profile of myofibroblasts. Hum Pathol 2008;39:846-56.
27. Lestou VS, O'Connell JX, Ludkovski O, et al. Coamplification of 12p11 and 12q13 approximately q22 in multiple ring chromosomes in a spindle cell sarcoma resolved by novel multicolor fluorescence in situ hybridization analysis. Cancer Genet Cytogenet 2002;139:44-7.
28. Colombo C, Urbini M, Astolfi A, et al. Novel intragenic large deletions of CTNNB1 gene identified in WT desmoid-type fibromatosis. Genes Chromosomes Cancer 2018;57:495-503.
29. Patel RM, Downs-Kelly E, Dandekar MN, et al. FUS (16p11) gene rearrangement as detected by fluorescence in-situ hybridization in cutaneous low-grade fibromyxoid sarcoma: a potential diagnostic tool. Am J Dermatopathol 2011;33:140-3.
30. Guo Y, Hao Y, Guan G. Low-grade fibromyxoid sarcoma in the middle ear as a rare location: a case report. Transl Pediatr 2022;11:1034-9.
31. Cai C, Dehner LP, El-Mofty SK. In myofibroblastic sarcomas of the head and neck, mitotic activity and necrosis define grade: a case study and literature review. Virchows Arch 2013;463:827-36.
32. Kim JH, Choi W, Cho HS, et al. Surgical treatment and long-term outcomes of low-grade myofibroblastic sarcoma: a single-center case series of 15 patients. World J Surg Oncol 2021;19:339.
33. Italiano A, Di Mauro I, Rapp J, et al. Clinical effect of molecular methods in sarcoma diagnosis (GENSARC): a prospective, multicentre, observational study. Lancet Oncol 2016;17:532-8.

Cite this article as: Zhu M, Cheng W, Liu X, Ma L, Chen Y. Enhanced magnetic resonance imaging features and management principles of low-grade myofibroblastic sarcoma of the breast: a case report. Gland Surg 2025;14(1):82-89. doi: 10.21037/gs-24-347